



~~SECRET~~ Livermore National Laboratory  
UNCLASSIFIED 21

DEFENSE TECHNOLOGIES ENGINEERING DIVISION

December 8, 1993

**Redacted version**

Mr. Gerry W. Johnson  
Area Manager (Acting),  
Amarillo Area Office  
U.S. Department of Energy  
P.O. Box 30030  
Amarillo, TX 79120

Dear Gerry:

Enclosed is the second of two key reports related to the W48 cracked pit incident. This report, with the transmittal letter attached, addresses the issue of high explosive reaction if a W48 pit cracked with the full high explosive charge present.

This report is provided for you and your staff's information. A copy is also being sent to Bill Weinreich at Mason & Hanger. The reports original distribution to DOE/AL, DOE/DP-6, and DOE/DP-20 is as shown. In addition, another copy was provided to Mr. Daniel Rhoades, DP-6.2 and it was my understanding that copy was being forwarded to the Defense Nuclear Facilities Safety Board.

I believe two copies of the first report, "Final Report on the W48 Cracked Pit Failure and Analysis and Recommendations", COMW-93-0285, are on the Pantex plant site and have been available to both DOE and Mason and Hanger at various times.

If you feel further information is needed, please contact me.

Sincerely,

Lee M. MacLean  
Associate Deputy Associate Director  
for Weaponization

LMM:kg  
h93-088

Attachments

The document transmitted herewith  
contains Restricted Data.

WHEN SEPARATED FROM ENCLOSURES, HANDLE  
THIS DOCUMENT AS unclassified

UNCLASSIFIED

~~SECRET~~



~~CONFIDENTIAL~~  
Lawrence Livermore  
DEFENSE TECHNOLOGIES

UNCLASSIFIED

THIS DOCUMENT CONSISTS OF  
110

Stephen J. Guidice, OOW  
U.S. Department of Energy  
Albuquerque Field Office  
P.O. Box 5400  
Albuquerque, NM 87185-5400

Attn: Richard Gonzales, WPD

Subject: Response of W48 Warhead High Explosive to a Pit Cracking Incident (U)

As part of LLNL's analysis of the W48 pit cracking incident, we have been considering the consequences of a similar incident, if it occurred while the full main charge high explosive was present. The results of our analysis clearly show that a failure of the W48's pit shell or weld will not initiate any high explosive reaction.

The enclosed report, "W48 High Explosive Response from Weld Joint Failure," presents the results of our analysis. In this analysis, we examined the delivery of energy to the high explosive and made comparisons to thresholds for several initiation mechanisms of the high explosive. The initiation mechanisms considered included:

- shock initiation
- energy delivered by frictional work to the surface of the high explosive
- internal energy delivered by flow of the high explosive
- pinching high explosive in the crack

We examined two configuration, that encompassed the pit and full high explosive configuration. The first configuration, representative of the full warhead, included the projectile case external to the high explosive. The second configuration, representative of an intermediate dismantlement stage, excluded the projectile case. We found that the first configuration, including the projectile case, was the most sensitive situation and thus was the controlling configuration.

UNCLASSIFIED

RESTRICTED DATA

This document contains restricted data as

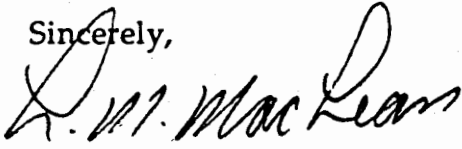
~~CONFIDENTIAL~~  
Derivative

~~CONFIDENTIAL~~  
UNCLASSIFIED

...baseline case, that shock initiation failed to reach high  
...thresholds by a factor greater than 100. Frictional work was a  
...initiation levels. Analysis shows there is no flow of high  
...the crack or extrusion into the crack thus eliminating flow work or  
...as sources of initiation.

In order to check the sensitivity of these results, we created an unrealistic model,  
capable of storing more energy than the baseline model. We increased material  
property constants of both the [redacted] and plutonium to physically impossible  
levels, that effectively delivered 80 times the energy to the high explosive of the  
baseline case. At this extreme condition, ignition thresholds were not reached for  
shock or frictional work mechanisms, positive margins were maintained, and no  
low or extrusion of high explosive occurs. It is clear that failure of the  
hell or weld in a W48 warhead cannot deliver sufficient energy to produce any  
high explosive reaction by these identified initiation mechanisms.

Sincerely,



L. M. MacLean  
Assistant Deputy Associate Director  
for Weaponization

MM:kg  
3-059

closure

distribution:

- phen J. Guidice, DOE/AL, OOW #2072
- Attn: Richard F. Gonzales, WPD
- m. Charles J. Beers, Jr., DOE/GTN, DP-20, #2145
- attn: Thomas J. Goodwin, DOE/GTN, DP-251
- tor Stello, Jr., DOE/GTN, DP-6, #2145
- attn: Daniel R. Rhoades, DOE/GTN, DP-65
- A. Bailey, L-125 w/o enclosure
- i. Clough, L-125 w/o enclosure
- H. Hubbell, L-125 w/o enclosure
- f. MacLean, L-125 w/o enclosure

- Gerry W. Johnson, AAO, #2075
- William A. Weinreich, M&H, #1390
- J. Thomas McGee, LLNL, PX, #1390

UNCLASSIFIED

~~CONFIDENTIAL~~

UNCLASSIFIED

CLASSIFIED DOCUMENT CONTROL SYSTEM

RECEIVED: Y DESTROYED: N TRANSMITTED: N

ORIGINATED: N REPRODUCED: N CLASSIFICATION CHG:

=====  
CRC NUMBER: 13-0041

DOC #: COMW-93-02

=====  
PAGES: 28

NUMBER OF COPIES: 1 COPY NUMBER: 1 SERIES: N/A

DATE RECEIVED: 12\17\1993 SENDER OR RECIPIENT: LAWRENCE  
LIVERMORE NAT'L

DOCUMENT DATE: 05\21\1993 MASON & HANGER DEPT:

TYPE OF DOCUMENT: REPORT CATEGORY: SRD

SUBJECT OR TITLE: W48 HIGH EXPLOSIVE RESPONSE FROM WELD JOINT  
FAILURE (U)

FILE NUMBER: Pick-up File !

YEAR: 1993

ASSIGNMENT:

TYPE OF FILE: VAULT FILE

PERSON RECEIVING: KIGHT

PERSON LOGGING: KIGHT

REMARKS:

UNCLASSIFIED

~~SECRET~~ ~~SECRET~~

UNCLASSIFIED

COMW-93-0284

THIS DOCUMENT CONSISTS OF 28

Lawrence Livermore National Laboratory  
Defense Technologies Engineering Division

### W48 High Explosive Response from Weld Joint Failure (U)

Daniel L. Lewis  
Steven K. Chidester  
Robert A. Bailey

Advanced Engineering Analysis Group

0002:DLL

#### Internal Distribution

R.A. Bailey	L-125
S.K. Chidester	L-125
R.B. Clough/W.M. Ploeger	L-125
D.B. Frischknecht	L-125
J.G. Green	L-328 (COC)
W.H. Hubbell	L-125
J. Lewis	L-125
W. MacLean	L-125
J. Streit	L-125

Original Conv

#### External Distribution

Stephen J. Guidice, DOE/AL, OOW #2072  
 Attn: Richard F. Gonzales, WPD  
 Adm. Charles Beers, Jr., DOE/GTN, DP-20, #2145  
 Attn: Thomas J. Goodwin, DOE/GTN, DP-251  
 Victor Stello, Jr., DOE/GTN, DP-6, #2145  
 Attn: Daniel R. Rhoades, DOE/GTN, DP-65  
 Al Nichols, WPD  
 Daniel R. Rhoades, DOE/GTN, DP-6.2, #2145  
 Gerry W. Johnson, AAO, #2075  
 William A. Weinreich, M&H, #1390  
 J. Thomas McGee, LLND

~~RESTRICTED DATA~~  
This document contains restricted data as defined in the Atomic Energy Act of 1954. Unauthorized disclosure is subject to administrative and Criminal Sanctions.

Derivative  
Classifier:

(Robert A. Bailey, Group Leader  
Defense Technologies Engineering Division, LLND)

~~SECRET~~ UNCLASSIFIED

## Summary

The work presented in this report clearly shows that a failure of the W48 pit's material, while W48 the pit is in the weapon geometry or any dismantlement state where the PBX-9404 high explosive surrounds the W48 pit, will not initiate a high explosive reaction. We examined the energy delivery processes to the high explosive that could initiate the high explosive and compared the energy delivery of such a failure to known initiation mechanisms for the high explosive. In particular we examined:

- direct shock initiation to the high explosive both axial and laterally,
- frictional work delivered to the high explosive as the crack slides across the high explosive,
- the flow of the high explosive and
- the pinching high explosive in the crack.

We used models that were very conservative in terms of maximizing the energy available and the energy delivery to the high explosive. As stated above, based on the work presented in this report, the high explosive will not react from the cracking

The W48 was modeled and analyzed to evaluate the response of the PBX-9404 high explosive to a failure of the weld joint at the waist of the pit due to differential thermal expansion. The analysis was performed for the W48 weapon geometry and for the pit/high explosive assembly after it has been removed from the outer case during dismantlement. Worst case conditions were used for all models by minimizing the interface gaps.

Due to the course meshing of the weld joint, the calculated failure temperatures are higher than have been calculated using a much more detailed nit model that does not include the high explosive<sup>1</sup>. This allows for greater storage of energy prior to failure, producing a conservative prediction of potential high explosive reactions. The failure of the weld joint imparts a pressure shock to the high explosive, but for the full W48 geometry this shock is two orders of magnitude below the minimum shock necessary to initiate a high explosive reaction. The frictional work imparted to the high explosive as the crack opens, is less than 6% of the work required to initiate a high explosive reaction. Also considered were the reaction mechanisms of flowing the high explosive past the shell, but the analysis indicates that the high explosive does not flow past the shell. Additionally, the analysis shows that the high explosive does not extrude into the crack thus prohibiting the pinching of the high explosive in the crack. Finally, we examined the applicability of the high explosive skid test data.

## W48 Description

The geometry of the W48 assembly was taken from the production piece part drawings for the W48 weapon system as defined in LLNL drawing AAA87-102889-OB<sup>2</sup> and is shown in Figure 1.

### Finite Element Models

Several different models were created to properly address the weld joint failure questions. First of all, there were two different stages of weapon dismantlement to be considered: 1) the weapon configuration, with the pit surrounded by the high explosive and inside the case, and 2) the pit surrounded by the high explosive, after removal of the case.

An finite element model for the weapon configuration was created from the geometry of Figure 1 using MAZE<sup>3</sup>, and the resulting mesh can be found in Figure 2. A few simplifications were made to the geometry of Figure 1 and they will not impact the results of this analysis. Since certain tolerance values could result in a full area contact between the two hemi-shells, this W48 model considered a single shell. This is conservative because it would tend to maximize the loads shell to the hemi-shells. Secondly, both the hemi-shells as solid throughout. The interface was modeled as a simple step joint as opposed to the complex geometry of the weld region and the interface stress relief areas. A close-up of the interface area, showing the mesh refinement, can be found in Figures 3 and 4. Finally, the model was truncated to eliminate any unneeded geometry away from the region of interest.

~~SECRET~~  
UNCLASSIFIED

COMW-93-0284  
Page 4

Figure 1

UNCLASSIFIED

~~SECRET~~



~~SECRET~~  
UNCLASSIFIED

COMW-93-0284  
Page 5

Figure 2

UNCLASSIFIED

~~SECRET~~

~~SECRET~~  
UNCLASSIFIED

COMW-93-0284  
Page 6

Figure 3

UNCLASSIFIED

~~SECRET~~

~~SECRET~~  
UNCLASSIFIED

COMW-93-0284  
Page 7

Figure 4

UNCLASSIFIED

~~SECRET~~

The nominal part contours were modified consistent with design tolerances to provide for a worst-case analysis, minimizing the interface gaps. Both [redacted] and the inner [redacted] were modeled in their maximum material conditions. The high explosive was modeled with a line-to-line fit [redacted]

The adhesive bond was not included in the model. The interface between the high explosive and the case was also modeled as a line-to-line fit.

with only one exception, all of the interfaces between the parts were modeled as sliding-with-void slidelines. The weld [redacted] was modeled with a tied-breaking slideline, providing both a tied slideline to model the weld and a method to model the weld failure. The tied-breaking slideline 'breaks' at individual nodes once a failure criterion has been reached. The failure criterion used by a tied-breaking slideline compares the average effective plastic strain of the material across the slideline to a user-defined threshold value. This slideline type [redacted]

(see Figure 3) which corresponds to a depth of weld [redacted] For simplicity, the material [redacted] was modeled only as [redacted]

The weapon configuration model, described above, was modified to create the other model. This was done simply by eliminating outer geometry as appropriate. The effective plastic strain failure criterion for the tied-breaking slideline was also adjusted to produce a maximum principal stress at failure of [redacted]. Selection of the failure criterion value is covered in the Finite Element Analysis section.

The models were changed slightly to include shrinkage [redacted] of the joint during the welding process. [redacted]

All else [redacted]

remained the same for each model, including the failure criterion for the respective tied-breaking slidelines.

Temperature was the only loading condition applied to the model. The temperature loading curve that was used for the analysis is given in Table 1. It begins at room temperature, the temperature at which the parts were made, and is increased [redacted] to 150°C. The temperature profile is assumed to be uniform over the entire model. Detailed thermal analysis has shown a slight temperature profile within the pit, however this would not alter the response of the system<sup>4</sup>. The chosen peak temperature of 150°C was more than adequate for the purpose of this analysis.

**Table 1**  
Temperature Loading Curve

Time (s)	0	20	150	1000
Temp (°C)	20	20	150	150

Material Parameters

the NIKE2D<sup>5</sup> material parameters used throughout the analysis are given in the tables below.

Table 2

~~SECRET~~

UNCLASSIFIED

Table 3



Table 4

Material Input Parameters - Material Type 12

Density (lb/in <sup>3</sup> )	Temp. (°C)	E (Msi)	Poisson's Ratio	CTE (μin/in°C)	Hard. Coeff. (ksi)	Hard. Exp.
Explosive 0.0689	20	0.864	0.29	36.5	16.7	0.562
	110	0.264	0.40	44.2	16.7	0.562
	700	0.264	0.40	44.2	16.7	0.562

~~SECRET~~

UNCLASSIFIED

### Element Analysis

...to differential thermal expansion were calculated using NIKE2D and post-processing using ORION<sup>8</sup>. All analysis was performed utilizing the dynamics option of the code with sufficient time step reduction to capture dynamic effects. The time step was 1.0E-08 seconds in the range of the weld joint failure to evaluate the magnitude of the ... to the high explosive from the failure of the weld joint.

...analysis showed that as the temperature is increased, the plutonium expands freely ... contact is made.

... causing tensile loading in the weld ... the tensile loading of the weld joint ... the use of maximum principal stress to predict failure in the weld material. But, as was ... in the Finite Element Models section, the failure criterion for a tied-breaking slideline ... used to model the weld joint is related to the average effective plastic strain across the ... Therefore, an appropriate effective plastic strain value needed to be determined for each ... order to properly calculate the weld failure.

... joint failure criteria for the two stages of dismantlement were established from initial runs ... model using a tied slideline in place of the tied-breaking slideline. The results from the ... were studied to determine the expected failure point of the weld joint, based on the ... principal stresses.

... The values of the effective plastic strain that ... to failure, based on the maximum principal stresses, were placed into the tied- ... slideline failure criterion for their respective models.

... In all cases, the ... tied-breaking slidelines did 'break' at their pre-determined failure stresses.

... results for the first model, the weapon configuration, are discussed in detail, while the results ... other models are simply presented due to the fact that their overall data trends are very ... However, significant findings from the analysis of the other models are also described in ... detail. Figure 5 shows the radial displacements

... The differing slopes indicate the different CTE values of the ... materials, ... The change ... that ... at ~75°C characterizes the contact

... consistent with detailed analysis which was done on only the bare pit<sup>9</sup>. The ... expansion continues, increasing the stresses in the weld, until the weld fails.

... Figure 6 provides a close-up view of the weld region, showing the maximum principal stress ... distribution ... during failure. Inspection of this figure, with comparison to ... Figure 3, reveals that the two inner nodes of the weld joint have already failed and the failure is ... propagating through the weld region. Figure 7 shows this same plot after complete failure of the ... joint, just two time steps later. Evidence of bending can be seen in the weld region along ... its corresponding pull-in effect.

~~SECRET~~

UNCLASSIFIED

COMW-93-0284  
Page 12

Figure 5

UNCLASSIFIED

~~SECRET~~



~~SECRET~~  
UNCLASSIFIED

COMW-93-0284  
Page 13

Figure 6

UNCLASSIFIED

~~SECRET~~

~~SECRET~~  
UNCLASSIFIED

COMW-93-0284  
Page 14

Figure 7

UNCLASSIFIED

~~SECRET~~

The stored energy that is released during the weld failure and imparted to the high explosive is of concern. Upon failure of the weld joint, the step joint geometry is such that it does not allow directly imparting all of the stored energy. The shells slide apart, dissipating some of the energy through friction and slowing the overall failure process.

A temperature (time) history is given in Figure 8. The specific nodes were selected because of their locations and the fact that the largest pressure shocks, due to the weld failure, occur in these regions.

Figure 8 also indicates that there are seemingly very large pressure increases upon weld failure with a maximum pressure of ~1900 psi. This pressure, however, consists of two components: static pressure, due to differential thermal expansion, and a pressure shock resulting from the energy released by failure of the weld joint.

This is more evident from inspecting the close-up view found in Figure 9 which shows that the true pressure shock is only ~400 psi. The effect of this pressure shock to the high explosive will be covered in the High Explosive Response section. As is expected, the figures show a drop in pressure for curve c, the node immediately adjacent to the joint interface upon joint separation.

When adjusting the models for weld shrinkage, the overall results for the two dismantlement stages vary only slightly from those described above.

The pressure shock to the high explosive is larger using the weld shrinkage geometry for the second stage. It reaches ~300 psi as compared to the ~200 psi for the previous model. Although this is a rather large percentage increase from the previous model, the magnitude is still rather small.

~~SECRET~~  
UNCLASSIFIED

COMW-93-0284  
Page 16

This model was then extended to look at failure of a bare pit. The calculated failure temperature from this model is the same. A much more detailed analysis of the pit alone resulted in a lower temperature,

However, this more detailed model included the actual weld material and the weld groove detail. Additionally, the prediction of a higher temperature in this analysis would result in conservatively high prediction of the peak shock pressure because of the additional energy stored in the pit.

UNCLASSIFIED

~~SECRET~~

~~SECRET~~  
UNCLASSIFIED

COMW-93-0284  
Page 17

Figure 8

UNCLASSIFIED

~~SECRET~~

~~SECRET~~  
UNCLASSIFIED

Figure 9

UNCLASSIFIED

~~SECRET~~

~~SECRET~~

UNCLASSIFIED

COMW-93-0284  
Page 19

Figure 10

UNCLASSIFIED

~~SECRET~~

~~SECRET~~

COMW-93-0284  
Page 20

UNCLASSIFIED

Figure 11

~~UNCLASSIFIED~~

~~SECRET~~



~~SECRET~~

COMW-93-0284  
Page 21

UNCLASSIFIED

Figure 12

~~UNCLASSIFIED~~

~~SECRET~~

~~SECRET~~

UNCLASSIFIED

Figure 13

UNCLASSIFIED

~~SECRET~~

~~SECRET~~

UNCLASSIFIED

### High Explosive Pressure Shock (Bounding Case)

The pressure shock imparted to the high explosive from the weld joint failure is the major concern for this analysis and a bounding case needed to be evaluated. Analysis of the previous models showed that weld failure in the weapon configuration resulted in the greatest shock to the high explosive. For a first cut at bounding the problem, the model for the weapon configuration was used and the failure criterion (effective plastic strain to failure) for the tied-breaking slideline was increased by a factor of three. This was done to effectively increase the amount of stored energy to be released at failure of the weld joint.

The new model used the weapon configuration, along with the weld shrinkage geometry and its maximum material conditions, but with a slightly different material model for the plutonium and a different failure criterion for the tied-breaking slideline.

Results of the pressure shock to the high explosive can be found in Figure 14 to be ~1000 psi, an increase of only a factor of 2.5 over the results from using the realistic material properties and failure criterion.

UNCLASSIFIED

~~SECRET~~

~~SECRET~~  
UNCLASSIFIED

COMW-93-0284  
Page 24

Figure 14

UNCLASSIFIED

~~SECRET~~

## High Explosive Response

The impact response of PBX-9404 is well characterized<sup>11,12,13,14</sup> and shock initiation has never been observed below 3 kbar. Several hot-spot formation and ignition concepts were investigated for PBX-9404 by Lee and Tarver. One theory postulates that the high explosive reaction is caused by stagnation of microjets of material accelerated into rapidly closing voids as the shock front propagates over the irregular particles and voids of a granular explosive. This ignition mechanism was first postulated by Seely<sup>15</sup> and elaborated by Stresau and Kennedy<sup>16</sup>. Another model of hot-spot formation is based on the amount of plastic work required at void peripheries for dynamic void collapse<sup>17</sup>. There are other theories but none of them would account for PBX-9404 to react from a shock wave less than 3 kbar. The analysis showed that the maximum pressure on the high explosive would be, in the bounding case ~1000 psi (0.069 kbar). This shock pressure is 44 times smaller than the reaction threshold measured for PBX-9404. The safety factor for shock initiation for the actual W48 configuration is 109. It is clearly not possible that shock pressure initiation of the high explosive will occur from the breaking

Another reaction mechanism for conventional high explosives like PBX-9404 is caused by the explosive flowing past a metal material<sup>18</sup>. This flow is the basis of a work criterion for the high explosive reaction. The analysis of the W48 pit cracking indicates that the high explosive does not flow. The analysis shows no flowing of the high explosive and thus, there is no possibility of a high explosive reaction from this mechanism.

Skid tests were developed at AWRE in England to evaluate safety of high explosives. Others have developed a large data base with many high explosives including PBX-9404<sup>19,20,21</sup>. In addition to evaluating high explosives, the floor coverings of the work area were also studied<sup>22</sup>. In the LLNL-Pantex version of the skid test, the explosive is supported on a pendulum and allowed to swing down from preset heights and strike at an angle on a sand-coated steel target plate. This test gives the impact a sliding or skidding component as well as a vertical one. There are recorded detonations from PBX-9404 at impact angles of 14° and 45° at drop heights above one meter. In the analysis of the pit cracking there is no drop height because the high explosive is in physical contact

As shown in Figures 7 and 10, a gap does open allowing the outer surface of the pit to move past the high explosive. The analysis of the unrealistic bounding case and the W48 configuration indicate that the gap opens to 0.09" and 0.01", respectively. Assuming the high explosive is not cracked at the waist, there could be at most 0.045" movement for the unrealistic bounding case and 0.005" for the W48 configuration. The maximum total pressure on the high explosive in all cases when the weld joint fails is under 2000 psi (Figure 8, 9, 11, 12, 13, and 14). The friction work done on the PBX-9404 can be calculated using the equation:

$$W_F = F_N \mu_F d$$

where  $W_F$  is the frictional work,  $F_N$  is the normal force on the PBX-9404 surface,  $\mu_F$  is the coefficient of friction and  $d$  is the relative distance moved. The coefficient of friction can be conservatively estimated to be 0.5 when there is adiprene between the explosive and metal. Others have found the coefficient of friction for cast HMX in contact with sand/epoxy resin/steel to be 0.4.

Studies determining friction coefficients of explosives vary significantly<sup>23</sup> and are difficult to perform<sup>24</sup>. The reaction threshold for PBX-9404 was experimentally tested<sup>25</sup> to be 1 cal/cm<sup>2</sup>. The calculated value of friction work on the PBX-9404 in the unrealistic bounding case is 0.483 cal/cm<sup>2</sup> which yields a safety factor of approximately 2 using the 1.0 cal/cm<sup>2</sup> criterion. The frictional work calculated in the W48 configuration case is 0.054 cal/cm<sup>2</sup> which gives a safety factor of 18.5. The table below shows the margins from the analytical results.

Configuration	Factors of Safety	
	Shock Initiation	Frictional Work
W48 worst case full-up geometry	109	18
W48 without outer case	145	N/A
W48 unrealistic bounding case	44	2

The analysis shows that the high explosive does not extrude into the crack. The high explosive is expanding away from the pit because of thermal expansion. If the weapon cooled after cracking, then if something went into the crack it would be the adiprene adhesive not the high explosive; therefore, there is no chance the PBX-9404 could get pinched in the crack and detonate.

### Conclusions

From the analysis performed for the two stages of dismantlement, the weld joint at the waist of the W48 pit is expected to fail due to differential thermal expansion if the temperature reaches a sufficient level. However, the expected failure temperatures were not accurately determined in this analysis, because the weld region was not modeled in sufficient detail. The failure releases stored energy and imparts the energy to the high explosive in the form of a pressure shock. The shock, in the cases evaluated here, does not provide the energy required to cause a high explosive reaction.

~~SECRET~~  
UNCLASSIFIED

COMW-93-0284  
Page 27

## REFERENCES

- 1 MacLean, L.M., Hanafee, J.E. and Bailey, R.A., "Final Report on the W48 Cracked Pit Failure Analysis and Recommendation", LLNL COMW-93-0285, June 30, 1993.
- 2 Drawing AAA-87-102889-OB (CAD file W.W48.AAA.87-102889) was redrawn and reassembled by Ron Bettencourt using the original contours. The work was done under the direction of Bill Amerman and approved by Bill Hubbell. This drawing was created from original AEC production document 250099, revised October 17, 1969.
- 3 Hallquist, J. O., "MAZE - An Input Generator for DYNA2D and NIKE2D - Users Manual", UCID-19029, June 1983.
- 4 MacLean, L.M., Hanafee, J.E. and Bailey, R.A., "Final Report on the W48 Cracked Pit Failure Analysis and Recommendation", LLNL COMW-93-00285, June 30, 1993.
- 5 Engelmann, B. and Hallquist, J. O., "NIKE2D - A Nonlinear, Implicit, Two-Dimensional Finite Element Code for Solid Mechanics - Users Manual", UCRL-MA-105413, April 1991.
- 6 Schauer, D. A., "The Weapons Materials Data Book Part I", UCRL-14677, January 1966.
- 7 Schauer, D. A., "The Weapons Materials Data Book Part I", UCRL-14677, January 1966.
- 8 Hallquist, J. O., "ORION - An Interactive Color Post-Processor for Two Dimensional Finite Element Codes - Users Manual", UCID-19310, January 1982.
- 9 MacLean, L.M., Hanafee, J.E. and Bailey, R.A., "Final Report on the W48 Cracked Pit Failure Analysis and Recommendation", LLNL COMW-93-00285, June 30, 1993.
- 10 MacLean, L.M., Hanafee, J.E. and Bailey, R.A., "Final Report on the W48 Cracked Pit Failure Analysis and Recommendation", LLNL COMW-93-00285, June 30, 1993.
- 11 Liddiard, T.P., "The Initiation of Burning in High Explosives by Shock Waves", 4th Detonation Symposium, p. 487 (1965).
- 12 Lee, E.L. and Tarver, C.M., "Phenomenological Model of Shock Initiation in Heterogeneous Explosives", Phys. Fluids 23, p. 2362 (1980) and references cited therein.
- 13 Kipp, M.E., Nunziato, J.W., Setchell, R.E., and Walsh, E.K., 7th Detonation Symposium, p. 394 (1981).
- 14 Dobratz, B.M., "LLNL Explosive Handbook", LLNL Report No. UCRL-52997, Jan. 1985.
- 15 Seely, L.B., "Proceedings of 4th Electric Initiator Symposium", Franklin Institute, Philadelphia, PA, 1963.

~~SECRET~~

UNCLASSIFIED

~~SECRET~~  
UNCLASSIFIED

COMW-93-0284  
Page 28

- 16 Stresau, R.H. and Kennedy, J.E., 6th Symposium on Detonation, Office of Naval Research, p. 68, 1976.
- 17 Wackerle, J., Johnson, J.O. and Halleck, P.M., 6th Symposium on Detonation, Office of Naval Research, p. 20, 1976.
- 18 Chidester, S.K. and Green, L.G., "A Frictional Work Predictive Method for the Initiation of Solid High Explosives from Low Pressure Impacts", Selected for publication in 10th Detonation Symposium, July 12, 1993.
- 19 Green, L.G., Weston, A.M. and Van Velkinburg, J.H., "Mechanical Behavior of Plastic-Bonded Explosives Vertically Dropped on a Smooth, Rigid, Steel Target Surface", UCRL-51022, 1971.
- 20 Dyer, A.S. and Taylor, J.W., "Initiation of Detonation by Friction on a High Explosive Charge", 5th Symposium on Detonation, Office of Naval Research, p. 291-300, 1970.
- 21 Crutchmer, J.A., "Skid Sensitivity of As-Pressed PBX-9404", Mason & Hanger - Silas Mason Co., Pantex Plant, MHSMP-79-50, 1970.
- 22 Henry, R.E., "Evaluation of Floor Coverings for Explosive Work Areas", LLNL, UCID-16887, 1975.
- 23 Dobratz, B.M., "Properties of Chemical Explosives and Explosive Simulants", UCRL-51319, LLNL, July 1974.
- 24 Anderson, W.H., "Role of the Friction Coefficient in the Frictional Heating Ignition of Explosives", Propellants and Explosives 6, p. 17-23 (1981).
- 25 Green, L., Weston, A., VanVelkinburg, "Mechanical and Frictional Behavior of Skid Test Hemispherical Billets, LLNL, UCRL-51085 (1971).

~~SECRET~~

UNCLASSIFIED